Title: **Simulation of STM2 Straylight**

CI-No: 121 000

Prepared by:	H.Hartmann, J.Neubert	Date:	01.07.2007
Checked by:	S. Idler	Date:	06.07.2007
Product Assurance:	R. Stritter	Date:	09.07.07
Configuration Control:	W. Wietbrock	Date:	09.07.07
Project Management:	Dr. Fricke	Date:	09/07/2007

Issue	Date	Sheet	Description of Change	Release
1	1.7.2007		First issue	

Table of contents

1 Introduction

Due to the discrepancies found between EQM stray light test results and the corresponding prediction [RD1, RD2] additional specific stray light testing on STM has been performed [RD3]. These tests in the following are referred to as STM2 tests.

The STM2 tests were performed at the ESTEC test centre.[1] For the tests the Herschel flight cryostat was equipped with a mechanical thermal dummy of PACS FPU and the cryogenic qualification models of HIFI FPU and SPIRE FPU. Due to the absence of the PACS instrument the STM2 stray light measurement was performed with the SPIRE instrument only. Nevertheless, simulations were performed for both PACS and SPIRE stray light levels.

The following Figure 1 shows the Herschel-STM2 stray light test setup.

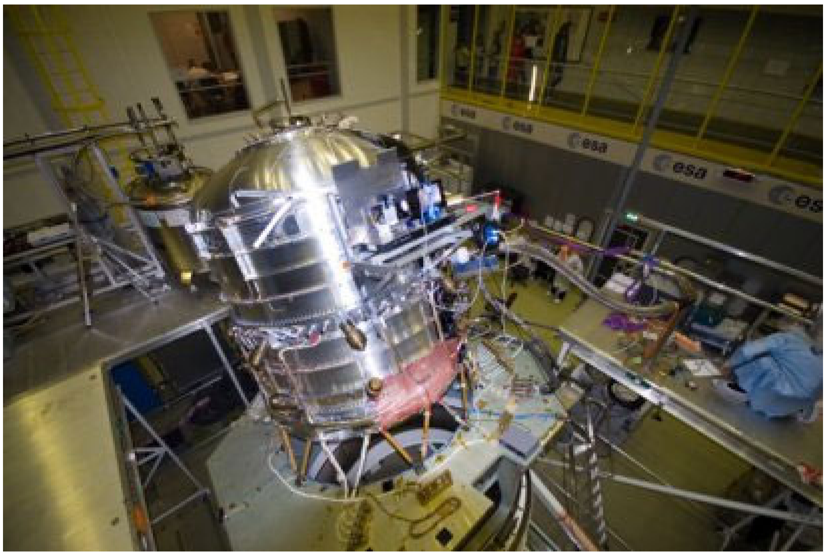

Figure 1 Herschel-STM2 stray light test[1]

[1] http://sci.esa.int/science-e/www/object/index.cfm?fobjectid=40172

2 Documents

2.1 Applicable Document

AD1	H-EPLM Requirements Specification (HERS)	H-P-2-ASPI-SP-0250, issue 3/3

2.2 Reference Document

RD1	Optical Configuration and Straylight during Ground Testing	HP-2-ASED-TN-0076, issue 2, 30.03.04
RD2	Explanations for excess EQM stray light	HP-2-ASED-AN-0020, 14.07.06
RD3	H-PLM STM2 Straylight Test Procedure	HP-2-TP-0110 issue 1, 6.10.06
RD4	Report on analysis of STM-2 straylight testing	HP-SPIRE-RAL-REP-002799, issue 1 12.01.07
RD5	H-PLM STM2 Straylight Test Report	HP-2-ASED-TR-0167, issue 1, 12.6.07
RD6	Herschel Straylight Calculation Results	HP-2-ASED-TN-0023, issue 4, 27.9.04

3 Abbreviations

ASAP	Advanced System Analysis Program
BRDF	Bidirectional Reflectance Distribution Function
CATIA	Computer Aided Three-Dimensional Interactive Application
CCM	Crycover Mirror
CVV	Cryostat vacuum vessel
ENB	Entrance baffle
FBI	Fractional Blackbody Integral
HBB	Hot black body
HIFI	Heterodyne Instrument for the Far-Infrared
IS	Instrument shield
K	Kelvin
LO	Local oscillator
LOU	Local oscillator unit
OB	Optical bench
PACS	Photodetector Array Camera and Spectrometer
SPIRE	Spectral and Photometric Imaging Receiver
STM	Structural and thermal model
TIS	Total Integrated Scatter
TS1	Thermal shield one
TS2	Thermal shield two
TS3	Thermal shield three
TSE	Thermal self-emission

4 Description of ASAP model configuration

For the simulation the stray light model has been updated to reflect the STM2 configuration. Compared to previous stray light predictions for the ground case [RD1], the following changes were introduced to the ASAP model:

- structural surfaces of the SPIRE entrance section are blackened,
- the cryocover mirror for STM is polished,
- the additional aperture in the entrance baffle (ENB) is added,
- TS1 baffle is added,
- vanes in TS2 baffle tubes are added

These design changes and the corresponding assumptions made in the ASAP model are described in the following. For details of the LO baffle model description see section 4.1, for changes made to other parts of the model see section 4.2 of this document.

The stray light test simulations cover the following test conditions as specified in RD3:

- Band 3 LO window is illuminated with a specific heat source (1473 K hot black body (HBB) with 20 mm diameter aperture located 379 mm in front of LO channel 3 window).
- The temperature of the Cryocover Mirror is varied.
- The temperatures of the Thermal Shields are varied.

The implemented model configuration is shown in the following figures.

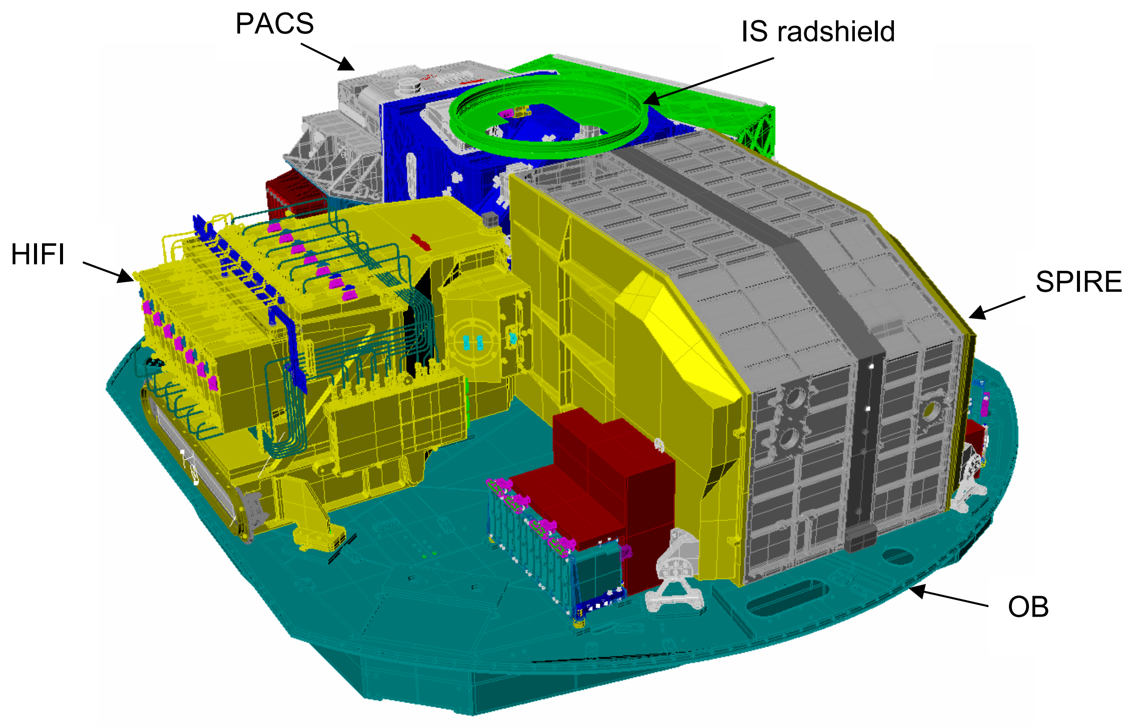

Figure 2 CAD model of the instruments HIFI, PACS and SPIRE mounted to the optical bench with the instrument shield (IS) radiation shield shown.

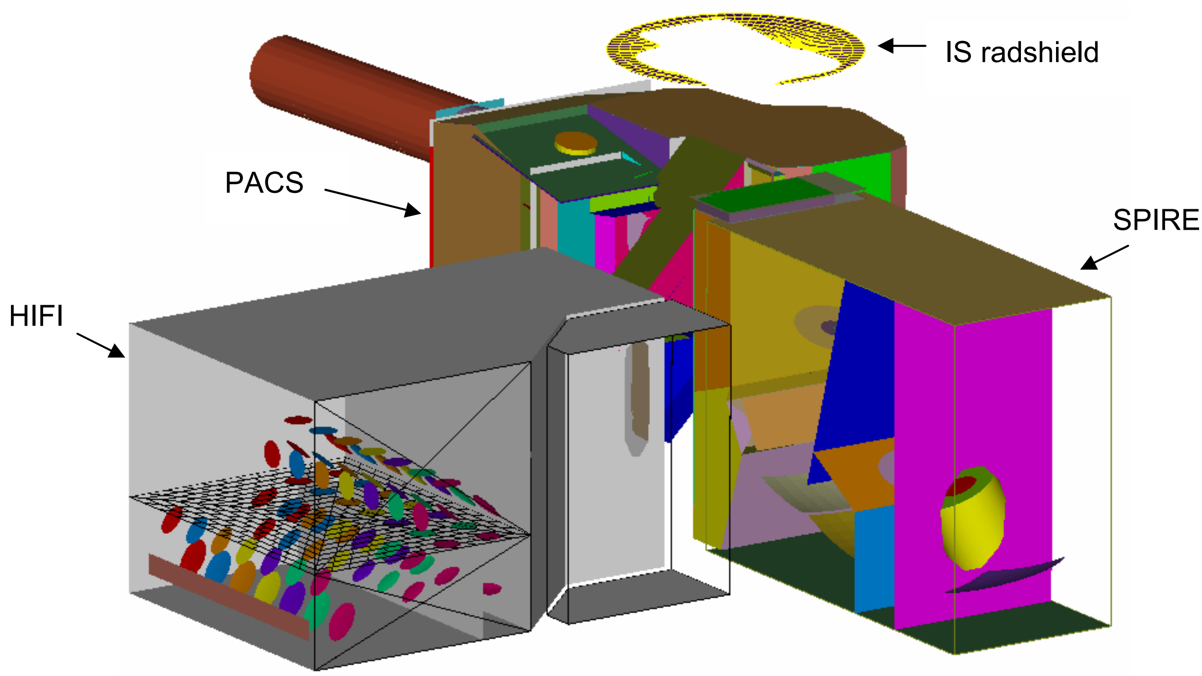

Figure 3 The instruments HIFI, PACS and SPIRE as implemented in the ASAP model with the IS radiation shield shown (LO baffle not shown).

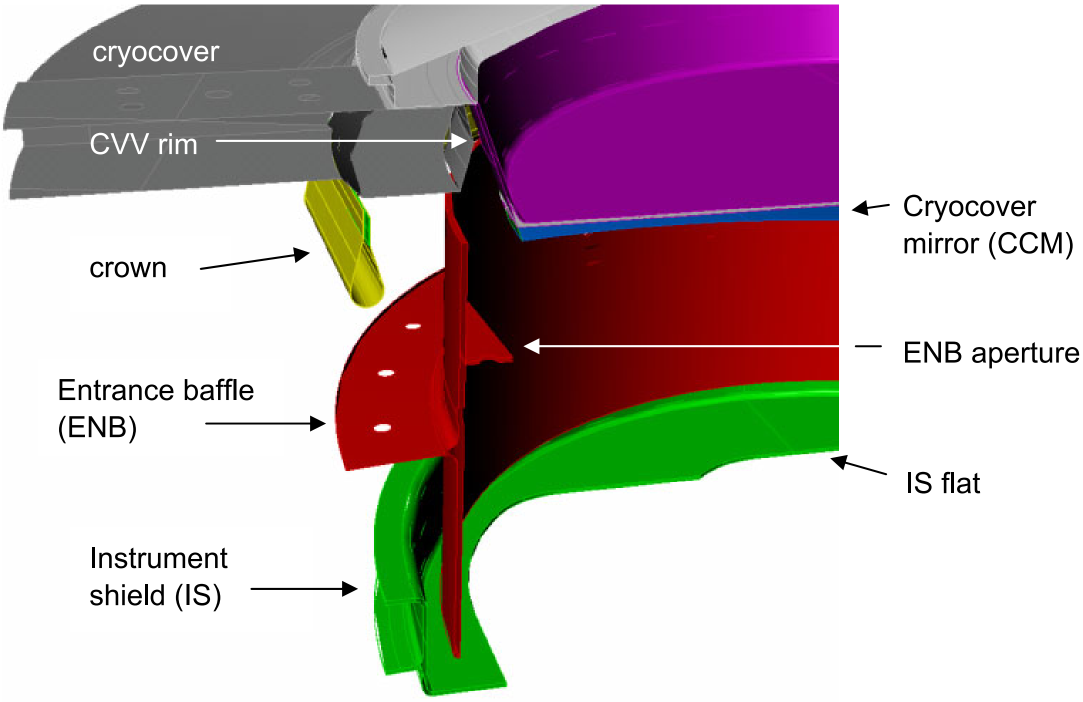

Figure 4 Cross sectional view through the cryostat cavity with the cryocover mirror closed (CAD model).

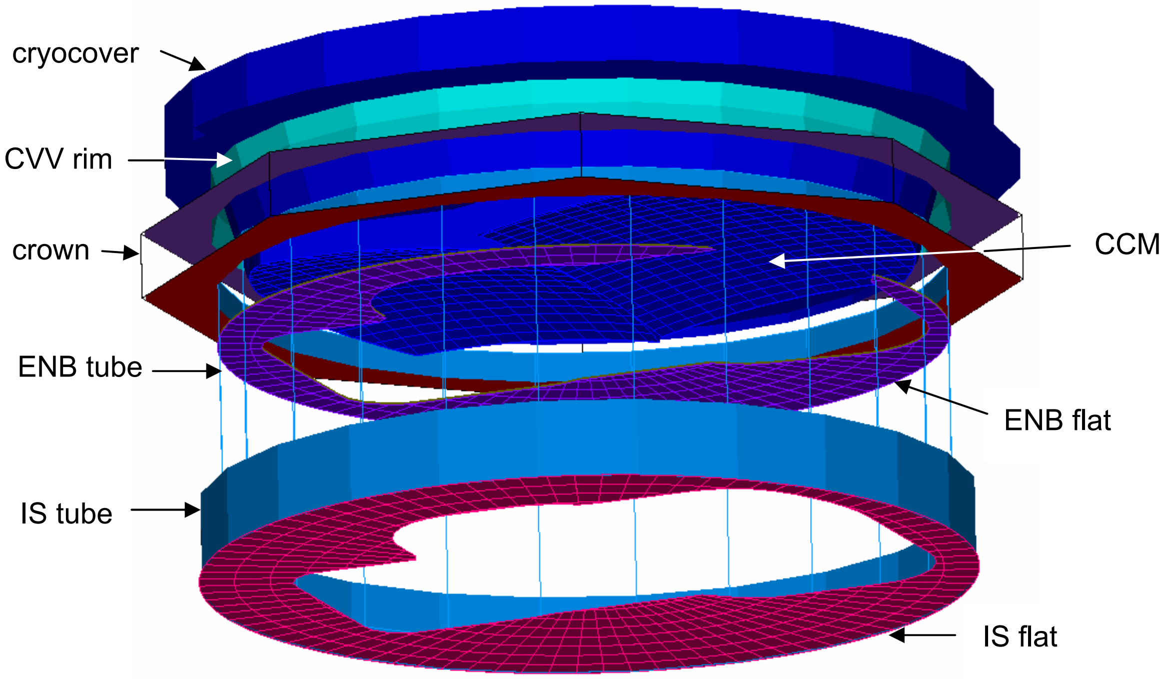

Figure 5 ASAP 3D plot of the cryostat cavity with closed cryocover mirror.

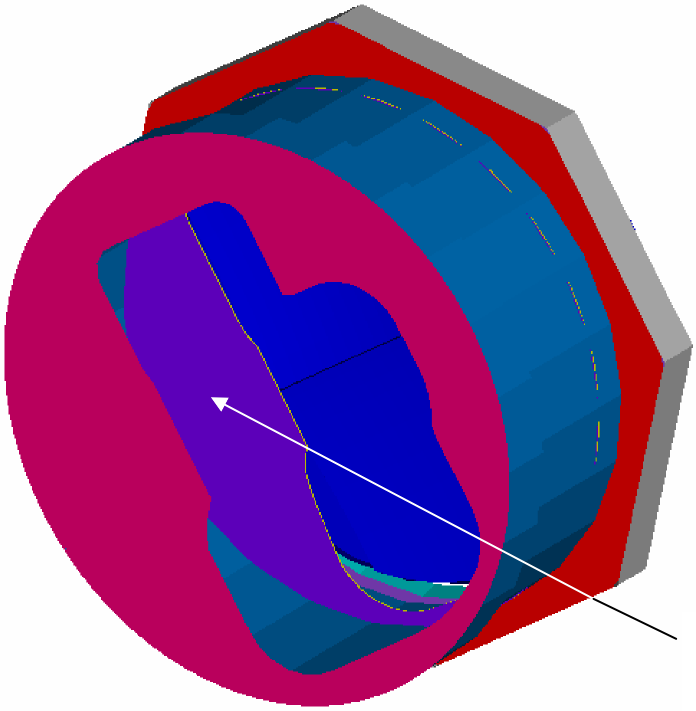

Figure 6 Details of the STM model configuration: Cryocover mirror, Crown, Entrance Baffle (baffle tube and the newly added aperture) and Instrument Shield Baffle (tube and aperture) are shown.

4.1 LO baffle model description and simulation results

The LO baffle ASAP model was initially implemented in a separate ASAP script This script can be used to calculate the power transfer from the LO windows as well as from an external hot blackbody source to the instrument shield (IS) openings.

The LO baffle model has then been integrated into the overall ASAP model of Herschel issue 5. This model now allows end to end simulations from the LO windows through HIFI and to the instrument detectors.

4.1.1 LO baffle model description

In the model the geometry as taken from a simplified CAD file is implemented. This file was derived directly from the current CATIA model and contains the interior and other surfaces relevant to the optical behaviour of the baffle. This geometry is shown in Figure 7.

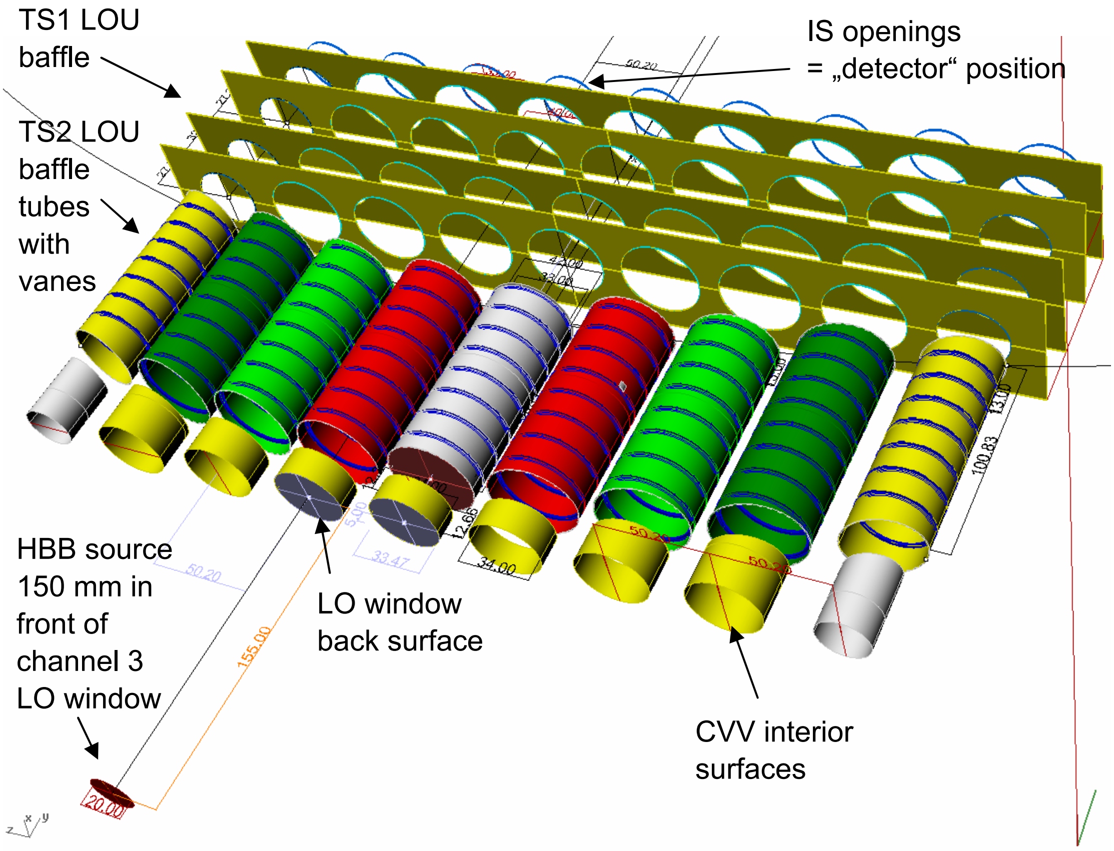

Figure 7 Simplified CAD model used to derive the geometry for the LO ASAP model. The HBB source is shown in front of LO channel 3. The distance to the LO window of channel 3 was increased during STM2 test from 155 mm to 379 mm.

The ASAP model is fully parameterized so that changes to the geometry or any optical properties can be done through assignments to the corresponding input parameters. These parameters and the commands defining the added geometry are contained in the macro LOU_BAFFLE[2].

The following Table 1 summarises the most important input parameters as used in the model.

[2] all changes made to the ASAP model (old filename H_iss4_2006_06.inr , new file name H_iss5_2007_06.inr) are documented in the excel sheet analysis_H_iss4_2006_06.inr.xls

Parameter and its value	comment
!! ray trace:	
LVL=3	number of times a scattered ray may be rescattered
LVLC=1.E-15	diffuse ray relative threshold, use LEVEL (LVL) (LVLC)
CTFF=1.E-12	absolute flux threshold, use CUTOFF (CTFF) (NCUT)
NCUT=100	maximum number of total object intersections for any ray
HLT=1000	maximum number of ray intersects on the same object, use HALT (HLT)
PTHFR=1E-5	flux sorting threshold, use PATHS TOTAL (PTHFR)
NRAY=500	source rays in one dimension
NSCAT=5	scattered rays per intersection
!! coatings:	
REFLECT=0.995	reflectivity ob metallic blank surfaces
R_BLACK=0.9	reflectivity of black anodyne surfaces
T_LOU_WIN=.96	transmission of LO windows
!! scatter models:	
HV_B=0.025	maximum BSDF (at specular), use HARVEY (HV_B) (HV_S) (HV_L)
HV_S=-0.5	asymptotic fall-off with angle
HV_L=0.01	A-Ao and B-Bo shoulder point in radians
!! geometry:	
!! TS1 baffle:	
A=70	half height on +/-Z side into Y
B=233	half length in Z
C=31	half length in X
D=55	half height on +/-X side into Y
E=-711.2	Y of outer horiz. surf.
F=30	distance between horiz. surfaces
!! TS2 baffle:	
TS2_AW_HW=33/2.	TS2 alignment window openings
TS2_LW_HW=40/2.	TS2 LO window openings
TS2_HOR_TILT=2	TS2 baffle surfaces tilt by 2 deg
!! CVV openings	
CVV_AW_HW=24/2	CVV alignment window openings
CVV_LW_HW=34/2	CVV LOU window openings
CVV_BT_Y1=-949.848	radius (around X) of CVV holes
CVV_BT_Y2=-962.511	Y min of CVV holes
RC=950	used for sources by H.H.
Y_DET_IS=-691.2	Y of DETector = Y of holes in IS
DHOLE=50.2	Z distance between tubes/channels
YHOLE5=-937.5	Y min of central (channel 4) TS2 baffle tube
DLY1=101.3	!! TS2 baffle vane Y positions
DLY2=106.8	…
DLY3=108.7	…
DLY4=111.3	…
DLY5=113.7	…
DLY6=DLY4	…
DLY5=113.7	…
RADHLL=21	TS2 LOU channel baffle tube inner radius
RADHLA=17.5	TS2 alignment channel baffle tube inner
VANE_D=2.	TS2 vane depths
HBB_HW=20/2	hot black body emitting radius

Table 1 Summary of input parameters to the LO baffle model.

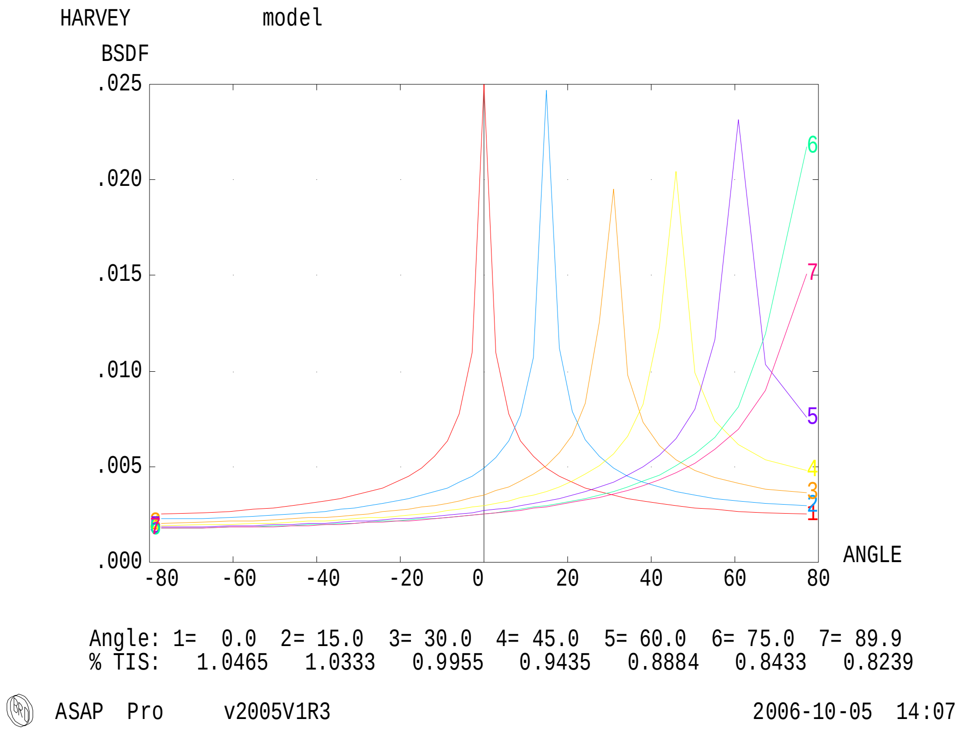

Figure 8 "HARVEY 0.025 -0.5 0.01" BRDF model (TIS=1% at normal incidence)

Figure 8 illustrates the scatter model used for the black anodised interior surfaces of TS1 and TS2 baffles. The reflectivity of these (in the VIS wavelength range) black surfaces is set to 90%. The CVV interior surfaces are left blank and therefore were assigned a reflectivity of 99.5%.

4.1.2 Simulation results for the hot black body source on LO band 3

This section deals with the LO baffle geometry as implemented in the ASAP model and simulation results obtained from it. The results calculated for the HBB source in front of channel 3 LO window are summarized in Table 2 of this section. The following figures illustrate the ray trace.

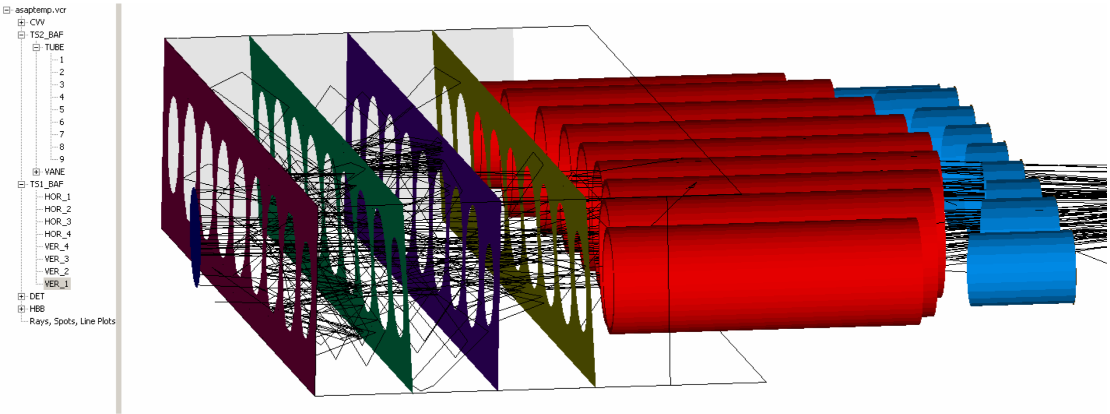

Figure 9 Ray trace with details of the TS1 LO baffle.

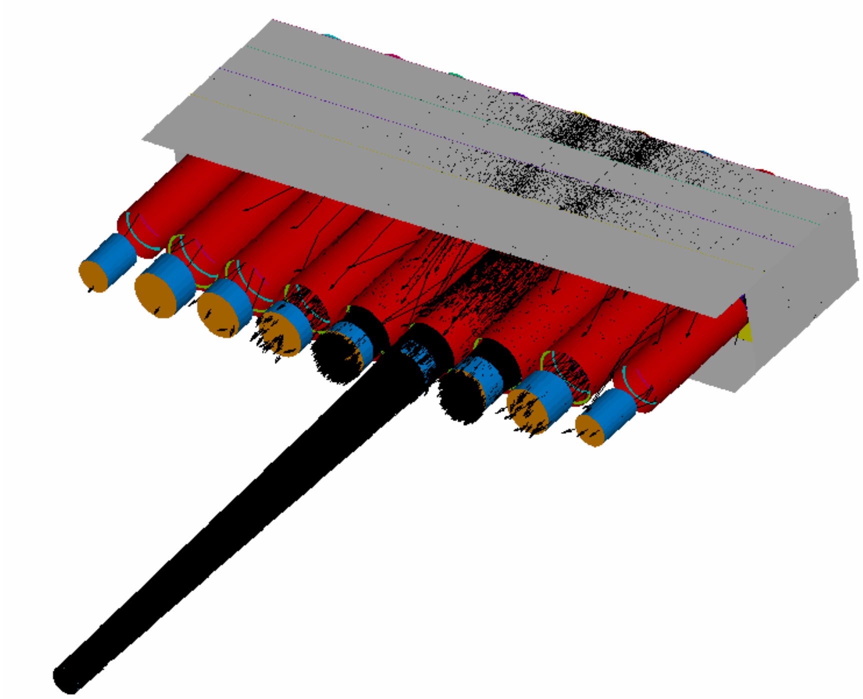

Figure 10 Ray trace in 3D with details of the TS1 LO baffle, HBB source located 379mm in front of channel 3 LO window.

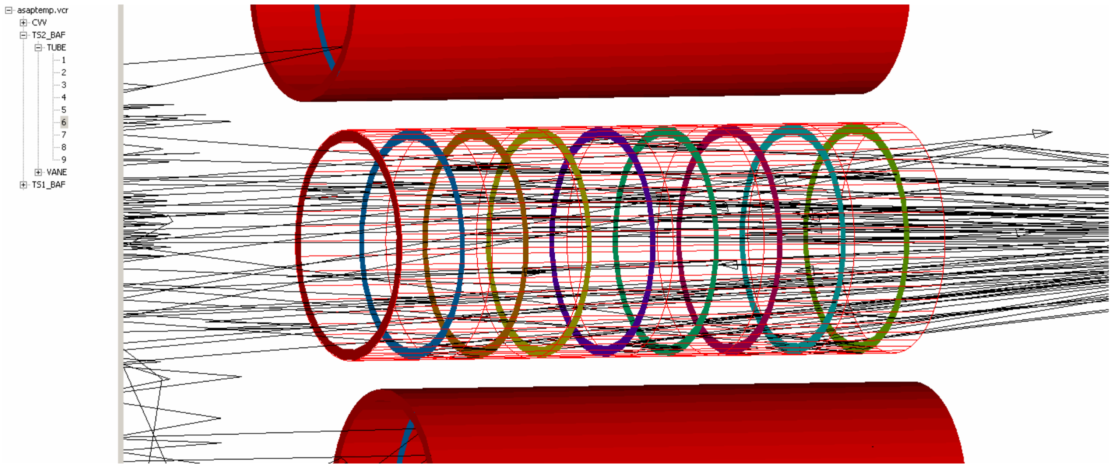

Figure 11 Ray trace with details of the TS2 LO baffle.

	Object	Rays	Flux	
115	3164	0.2079463E-05	DET.LOU_0	
116	16914	0.2136360E-04	DET.LOU_1	
117	125261	0.4305017E-03	DET.LOU_2	
118	881281	0.1020624	DET.LOU_3	
119	124440	0.4164304E-03	DET.LOU_4	
120	16587	0.2133241E-04	DET.LOU_5	
121	2566	0.1709802E-05	DET.LOU_6	
122	514	0.1781661E-06	DET.LOU_7	
123	182	0.7384871E-07	DET.LOU_8	
TOTAL	1170909	0.1029560		

FLI	314.1593
FLO	.102956
ATTENUATION	3.277E-4

Table 2 Results for the HBB source 379mm in front of band 3 LO window, IS openings named DET.LOU_?.

Table 2 shows results obtained for the simulation of the radiation transfer from a hot black body (HBB) source located 379 mm in front of LO window 3 through the LO baffle and to the instrument shield openings. The input flux (FLI) equals the emitting area in system units (mm^2), FLO is the total flux in all IS openings. The maximum occurs on channel 3 IS opening.

The attenuation of the HBB source within the baffle is 3.277×10^{-4}.

4.2 Further assumptions made in the simulations

The cryocover mirror has been polished and therefore is assigned a BRDF with slope -1.7 and the value of 0.73 at 0.01 radians (as assumed previously in RD1). The corresponding TIS value is 0.45%. For SPIRE wavelengths this assumption is considered conservative, the real BRDF for SPIRE might be even lower due to longer wavelengths of observation.

The cryocover mirror emissivity is assumed to be temperature dependent. The corresponding emissivities were adjusted according to the values given on page 22 of RD4.

The entrance section of SPIRE, i.e. the surfaces named POCKET, SIDE1MZ_UPPER, SIDE2PZ_UPPER, SIDE5PY_UPPER and SIDE6MY_UPPER in the ASAP code are assumed black with a total hemispherical reflectivity of 5%. All other structural surfaces are assumed to have a reflectivity of 95%.

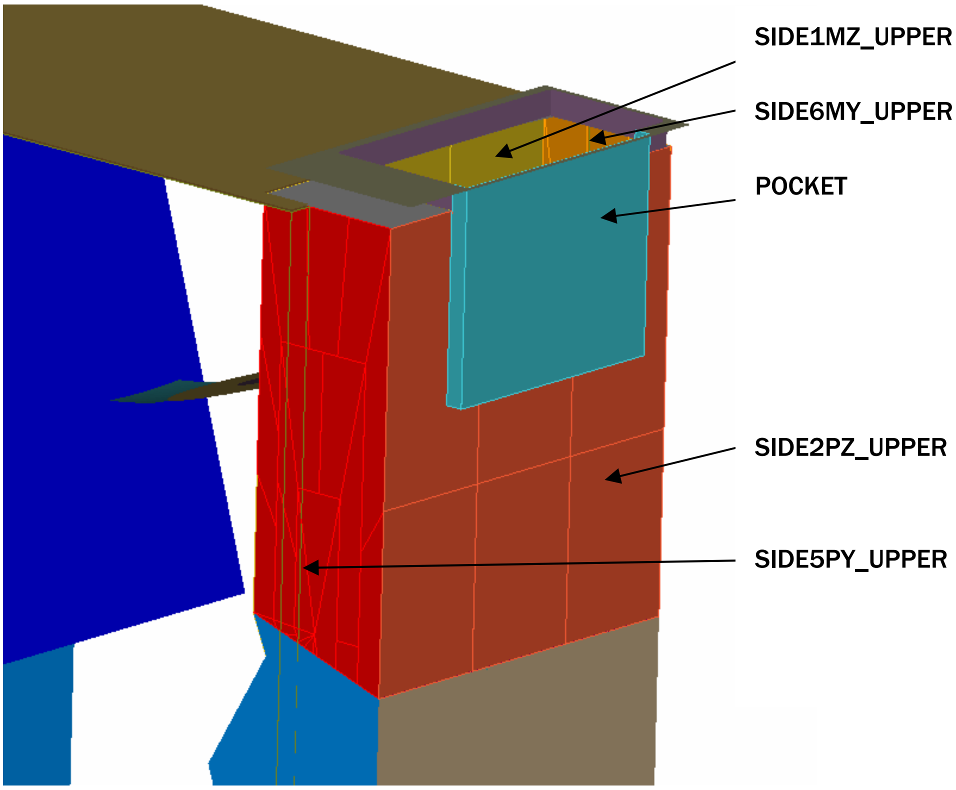

Figure 12 ASAP 3D plot of SPIRE entrance section showing which surfaces have been assumed to be “black”.

4.3 LO baffle integrated into the Herschel ASAP model

The ASAP model issue 5 with the integrated new LO baffle geometry allows the simulation of emission from an external hot black body source and from the LO windows traced through the system.[3]

The following figures illustrate the LO baffle added to the ASAP model.

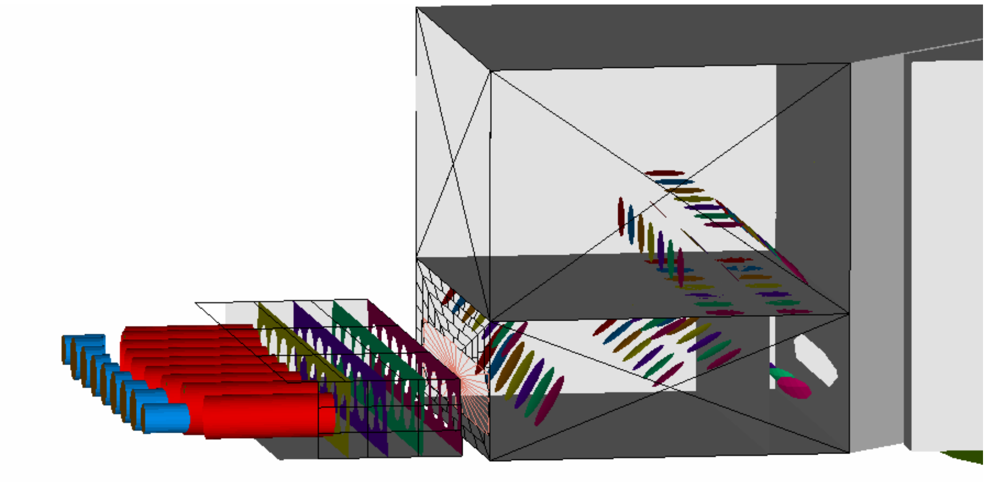

Figure 13 LO baffle as added to the Herschel ASAP model.

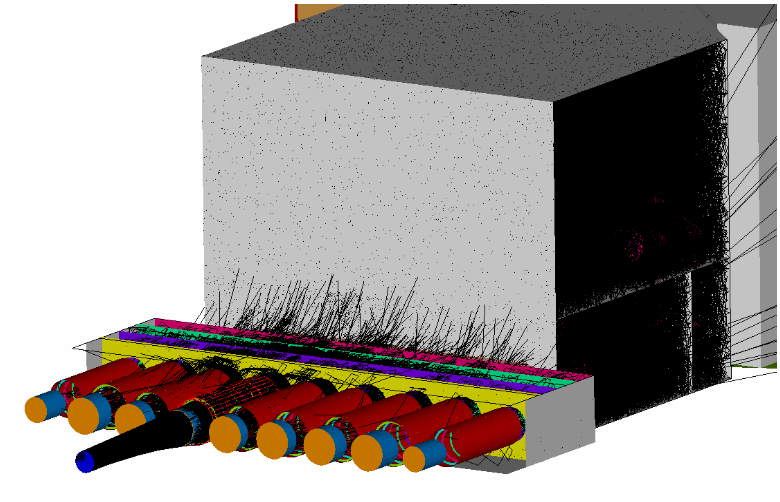

Figure 14 Raytrace from HBB source on LO channel 3, HIFI compartments shown with transparent sidewalls.

[3] the changes made to the model are documented in file analysis_H_iss4_2006_06.xls, the new ASAP script is stored under filename H_iss_5_2007_06.inr, the added TSE cases are available through parameters GRCASE=7 and XDIRECT=0 and XDIRECT=2.

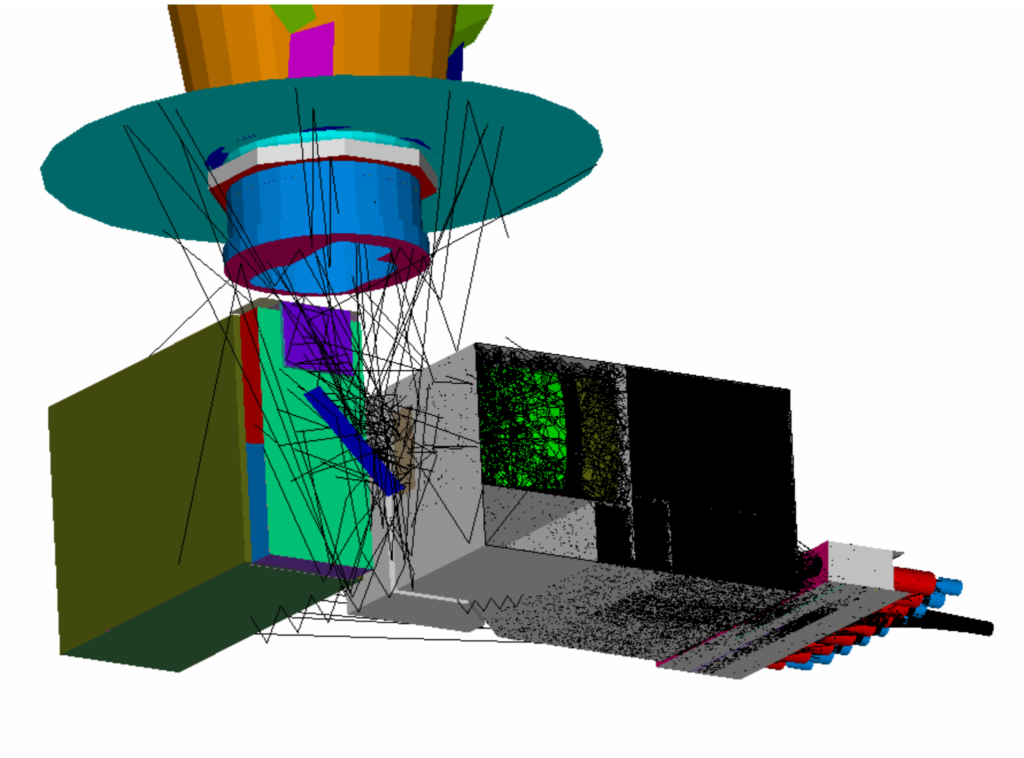

Figure 15 Raytrace from HBB source on LO channel 3, HIFI and SPIRE instruments shown.

4.4 Calculation of thermal self emission

As in previous stray light calculations the transfer of thermal self emission through the system was calculated in two steps:

1. calculation of effective source areas transferred to the detectors for each path by ray tracing
2. calculation of transferred power from the effective source areas and their summation in a separate Excel sheet[4]

In the following the formulas as used in the calculations according to step 2 are summarized:

According to Plank's law the spectral radiant emittance of a blackbody is[5]

$$W_{bb}(\lambda,T) = \frac{C_1}{\lambda^5}\frac{1}{e^{C_2/\lambda T}-1}$$ with $$C_1 = 3.74\cdot 10^4\ W\mu m^4/cm^2$$

$$C_2 = 1.44\cdot 10^4\ \mu m\, K$$

The "grey body" emits with

$$W_{gb}(\lambda,T) = \varepsilon(\lambda)\cdot W_{bb}(\lambda,T)$$ and emissivity $0 \le \varepsilon(\lambda) \le 1$

The detector only responds to a limited waveband. This can be taken into account through the spectral radiant emittance integrated over the detector waveband. To obtain this value the integral

$$FBI(\lambda\cdot T) = \frac{\int_0^{\lambda}\frac{1}{\lambda^5}\frac{1}{e^{C_2/\lambda T}-1}d\lambda}{\int_0^{\infty}\frac{1}{\lambda^5}\frac{1}{e^{C_2/\lambda T}-1}d\lambda}$$

has to be calculated. This integral equals the fraction of the blackbody radiant emittance in the detector wavelength interval $0 \ldots \lambda$.

ASAP provides a numerical solution to this integral through the FBI function (note $0 < FBI < 1$). Using the FBI function the grey body radiance into the waveband $\lambda_{\min} < \lambda < \lambda_{\max}$ can be expressed according to Stefan-Boltzman's law

$$L = \frac{\varepsilon\sigma T^4}{\pi}(FBI(\lambda_{\max}T) - FBI(\lambda_{\min}T))$$ with $$\sigma = 5.67\cdot 10^{-14}\frac{W}{mm^2K^4}$$

The expression for the irradiance of a grey body emitting into half-space is

$$E = \varepsilon\sigma T^4(FBI(\lambda_{\max}T) - FBI(\lambda_{\min}T))\quad .$$

This expression is used in the power calculations.

---

[4] the current version is stored in file TSE_Herschel_STM2_corr_11.xls

[5] see ASAP stray light tutorial notes and reference given therein: Richard D. Hudson, Infrared System Engineering, John Wiley and Sons, New York, 1969, p.35

5 Results of thermal self emission calculations

5.1 Static load cases

The test conditions during STM2 test are described in RD3. Test results can be found in RD4. The actual temperatures reached during the test were used as an input to the TSE power calculations for the static load cases and the results are given in Table 4 to Table 8. In these tables also the fractional blackbody integrals (FBI) and the resulting grey body irradiances [pW/mm^2] are listed. The calculated stray light levels on PACS and SPIRE detectors are given in pW (full field) and also as formerly agreed in % of standard telescope emission.
The following table summarizes the results obtained for the static load cases. The load cases are named according to table 3 of RD 5. The detector bands 88 µm, 177 µm (PACS), 230 µm, 550 µm and 670 µm (SPIRE) were calculated. The detector bandwidth is assumed to be $\lambda / \Delta\lambda = 3$.

case according to table 3 of RD5 :		static 1	static 2	static 3	static 4	static 5
PACS 88 µm band	**TSE in % st**	**1.11**	**1.02**	**11.15**	**84.71**	**4.89**
PACS 177 µm band	**TSE in % st**	**1.33**	**1.21**	**9.77**	**50.41**	**4.15**
SPIRE 230 µm band	**TSE in % st**	**3.14**	**2.93**	**14.54**	**58.59**	**7.62**
SPIRE 550 µm band	**TSE in % st**	**3.69**	**3.33**	**14.24**	**48.74**	**7.54**
SPIRE 670 µm band	**TSE in % st**	**3.83**	**3.42**	**14.24**	**47.64**	**7.61**

Table 3 Overview of predicted thermal self emission levels for the static load cases.

The following tables contain the detailed calculations as contained in excel sheet TSE_Herschel_STM2_corr_11.xls for the static load cases.

It is noted that the emission from the LO windows through HIFI FPU on the PACS and SPIRE sensors have been calculated in 2 ways:

1) 3 steps calculation with LO windows to FPU input by ray-tracing, FPU through put by worst case assumption (attenuation = 0.166), FPU output (from M3) to PACS/SPIRE sensors by ray-tracing.

2) 1 step calculation with ray-tracing from LO windows through all 7 HIFI FPU channels to PACS/SPIRE sensors.

Method 1) reveals much higher straylight then method 2), but for both methods the resulting straylight is negligible. For the overall straylight prediction the higher values from method 1) have been taken. The values from method 2) are listed in the tables as well for information.

case according to table 3 of RD4 : contributions to thermal self-emission	A eff [mm²]	GCF	ε [0..1]	static 1 T [K]	static 2 T [K]	static 3 T [K]	static 4 T [K]	static 5 T [K]
Standard telescope	4.47	1	0.0150					
temperature T [K]				70	70	70	70	70
FBI integral for PACS 88 µm band				1.68E-01	1.68E-01	1.68E-01	1.68E-01	1.68E-01
grey body irradiance [pW/mm^2]				3438.52	3438.52	3438.52	3438.52	3438.52
total flux at PACS detector [pW]				15356.42	15356.42	15356.42	15356.42	15356.42
% of standard telescope emission				100	100	100	100	100
Emission from CCM	2.26	1	ε [T]:	0.0010	0.0010	0.0013	0.0023	0.0010
temperature T [K]				11	5	86	199	13
FBI integral for PACS 88 µm band				1.17E-03	2.54E-09	1.23E-01	1.97E-02	5.18E-03
grey body irradiance [pW/mm^2]				9.73E-04	9.00E-11	502.38	4018.26	0.01
total flux at PACS detector [pW]				2.19E-03	2.03E-10	1133.37	9065.20	0.02
% of standard telescope emission				1.43E-05	1.32E-12	7.38	59.03	1.23E-04
Emission from warm CVV	6.09E-05	1	0.0433					
temperature T [K]				293	293	293	293	293
FBI integral for PACS 88 µm band				7.21E-03	7.21E-03	7.21E-03	7.21E-03	7.21E-03
grey body irradiance [pW/mm^2]				1.30E+05	1.30E+05	1.30E+05	1.30E+05	1.30E+05
total flux at PACS detector [pW]				7.9	7.9	7.9	7.9	7.9
% of standard telescope emission				0.052	0.052	0.052	0.052	0.052
Gap CVV / TS2 baffle (crown)	2.88E-04	1	0.0433					
temperature T [K]				40	38	38	75	80
FBI integral for PACS 88 µm band				2.42E-01	2.38E-01	2.38E-01	1.53E-01	1.38E-01
grey body irradiance [pW/mm^2]				1519.22	1217.00	1217.00	11860.46	13903.28
total flux at PACS detector [pW]				0.44	0.35	0.35	3.42	4.01
% of standard telescope emission				0.003	0.0023	0.0023	0.022	0.026
Emission from TS 2 Baffle tube	2.991E-03	1	0.4329					
temperature T [K]				40	38	38	75	80
FBI integral for PACS 88 µm band				2.42E-01	2.38E-01	2.38E-01	1.53E-01	1.38E-01
grey body irradiance [pW/mm^2]				1.52E+04	1.22E+04	1.22E+04	1.19E+05	1.39E+05
total flux at PACS detector [pW]				45.44	36.40	36.40	354.75	415.86
% of standard telescope emission				0.296	0.237	0.237	2.310	2.708
Emission from gap below IS	3.626E-03	1	0.9					
temperature T [K]				5.2	5.2	5.2	5.2	5.2
FBI integral for PACS 88 µm band				6.67E-09	6.67E-09	6.67E-09	6.67E-09	6.67E-09
grey body irradiance [pW/mm^2]				2.49E-07	2.49E-07	2.49E-07	2.49E-07	2.49E-07
total flux at PACS detector [pW]				9.02E-10	9.02E-10	9.02E-10	9.02E-10	9.02E-10
% of standard telescope emission				5.87E-12	5.87E-12	5.87E-12	5.87E-12	5.87E-12
Emission from Cryocover Mirror Tube	1.117E-04	1	0.4329					
temperature T [K]				5	5	86	199	13
FBI integral for PACS 88 µm band				2.54E-09	2.54E-09	1.23E-01	1.97E-02	5.18E-03
grey body irradiance [pW/mm^2]				3.90E-08	3.90E-08	164758.6	759609.4	3.63
total flux at PACS detector [pW]				4.35E-12	4.35E-12	18.41	84.86	0.000
% of standard telescope emission				2.84E-14	2.84E-14	0.12	0.6	2.64E-06
Gap between EB TUBE and IS TUBE	4.467E-04	1	0.4329					
temperature T [K]				40	38	38	75	80
FBI integral for PACS 88 µm band				2.42E-01	2.38E-01	2.38E-01	1.53E-01	1.38E-01
grey body irradiance [pW/mm^2]				1.52E+04	1.22E+04	1.22E+04	1.19E+05	1.39E+05
total flux at PACS detector [pW]				6.787	5.437	5.437	52.985	62.111
% of standard telescope emission				0.044	0.035	0.035	0.345	0.404

Table 4 (continued on next page)

LOU window emission through HiFi M3	2.892E-04	0.00046	0.9					
temperature T [K]				293	293	293	293	293
FBI integral for PACS 88 µm band				7.21E-03	7.21E-03	7.21E-03	7.21E-03	7.21E-03
grey body irradiance [pW/mm^2]				2.71E+06	2.71E+06	2.71E+06	2.71E+06	2.71E+06
total flux at PACS detector [pW]				0.3611	0.3611	0.3611	0.3611	0.3611
% of standard telescope emission				0.0024	0.0024	0.0024	0.0024	0.0024
LOU windows (all) through TS2/HIFI	5.82E-09	1	0.9					
temperature T [K]				293	293	293	293	293
FBI integral for PACS 88 µm band				7.21E-03	7.21E-03	7.21E-03	7.21E-03	7.21E-03
grey body irradiance [pW/mm^2]				2.71E+06	2.71E+06	2.71E+06	2.71E+06	2.71E+06
total flux at PACS detector [pW]				0.016	0.016	0.016	0.016	0.016
% of standard telescope emission				0.0001	0.0001	0.0001	0.0001	0.0001
Emission via gap below IS, holes in OB	3.626E-03	0.06285	0.9					
temperature T [K]				11	11	11	11	11
FBI integral for PACS 88 µm band				1.17E-03	1.17E-03	1.17E-03	1.17E-03	1.17E-03
grey body irradiance [pW/mm^2]				0.88	0.88	0.88	0.88	0.88
total flux at PACS detector [pW]				2.00E-04	2.00E-04	2.00E-04	2.00E-04	2.00E-04
% of standard telescope emission				1.30E-06	1.30E-06	1.30E-06	1.30E-06	1.30E-06
Emission from LOU via gap below IS	3.626E-03	0.00451	0.9					
temperature T [K]				293	293	293	293	293
FBI integral for PACS 88 µm band				7.21E-03	7.21E-03	7.21E-03	7.21E-03	7.21E-03
grey body irradiance [pW/mm^2]				2.71E+06	2.71E+06	2.71E+06	2.71E+06	2.71E+06
total flux at PACS detector [pW]				44.385	44.385	44.385	44.385	44.385
% of standard telescope emission				0.289	0.289	0.289	0.289	0.289
LOU via gap between ENB and IS	4.467E-04	0.01766	0.9					
temperature T [K]				293	293	293	293	293
FBI integral for PACS 88 µm band				7.21E-03	7.21E-03	7.21E-03	7.21E-03	7.21E-03
grey body irradiance [pW/mm^2]				2.71E+06	2.71E+06	2.71E+06	2.71E+06	2.71E+06
total flux at PACS detector [pW]				21.394	21.394	21.394	21.394	21.394
% of standard telescope emission				0.139	0.139	0.139	0.139	0.139
TSE flux at PACS full field [pW]				**126.8**	**116.3**	**1268.1**	**9635.3**	**556.1**
TSE in % of standard telescope				**0.83**	**0.76**	**8.26**	**62.74**	**3.62**
5% additional for diffraction				0.04	0.04	0.41	3.14	0.18
30% additional for misalignment				0.25	0.23	2.48	18.82	1.09
total TSE incl. diffr. + misalignm.				**1.11**	**1.02**	**11.15**	**84.71**	**4.89**

Table 4 continued: Thermal self emission contributors calculated for PACS 88 µm waveband.

case according to table 3 of RD4 : contributions to thermal self-emission	A eff [mm^2]	GCF	ε [0..1]	static 1 T [K]	static 2 T [K]	static 3 T [K]	static 4 T [K]	static 5 T [K]
Standard telescope	4.47	1	0.0150					
temperature T [K]				70	70	70	70	70
FBI integral for PACS 177 µm band				4.53E-02	4.53E-02	4.53E-02	4.53E-02	4.53E-02
grey body irradiance [pW/mm^2]				924.97	924.97	924.97	924.97	924.97
total flux at PACS detector [pW]				4130.91	4130.91	4130.91	4130.91	4130.91
% of standard telescope emission				100	100	100	100	100
Emission from CCM	2.26	1	ε [T]:	0.0010	0.0010	0.0013	0.0023	0.0010
temperature T [K]				11	5	86	199	13
FBI integral for PACS 177 µm band				9.29E-02	4.57E-04	2.79E-02	3.08E-03	1.47E-01
grey body irradiance [pW/mm^2]				7.71E-02	1.62E-05	114.21	626.99	0.24
total flux at PACS detector [pW]				1.74E-01	3.65E-05	257.65	1414.48	0.54
% of standard telescope emission				4.21E-03	8.85E-07	6.24	34.24	0.0130
Emission from warm CVV	6.09E-05	1	0.0433					
temperature T [K]				293	293	293	293	293
FBI integral for PACS 177 µm band				1.04E-03	1.04E-03	1.04E-03	1.04E-03	1.04E-03
grey body irradiance [pW/mm^2]				1.88E+04	1.88E+04	1.88E+04	1.88E+04	1.88E+04
total flux at PACS detector [pW]				1.142	1.142	1.142	1.142	1.142
% of standard telescope emission				0.028	0.028	0.028	0.028	0.028
Gap CVV / TS2 baffle (crown)	2.88E-04	1	0.0433					
temperature T [K]				40	38	38	75	80
FBI integral for PACS 177 µm band				1.37E-01	1.48E-01	1.48E-01	3.86E-02	3.32E-02
grey body irradiance [pW/mm^2]				8.61E+02	7.60E+02	7.60E+02	3.00E+03	3.34E+03
total flux at PACS detector [pW]				0.248	0.219	0.219	0.865	0.962
% of standard telescope emission				0.006	0.005	0.005	0.021	0.023
Emission from TS 2 Baffle tube	2.991E-03	1	0.4329					
temperature T [K]				40	38	38	75	80
FBI integral for PACS 177 µm band				1.37E-01	1.48E-01	1.48E-01	3.86E-02	3.32E-02
grey body irradiance [pW/mm^2]				8.61E+03	7.60E+03	7.60E+03	3.00E+04	3.34E+04
total flux at PACS detector [pW]				25.757	22.726	22.726	89.758	99.812
% of standard telescope emission				0.624	0.550	0.550	2.173	2.416
Emission from gap below IS	3.626E-03	1	0.9					
temperature T [K]				5.2	5.2	5.2	5.2	5.2
FBI integral for PACS 177 µm band				6.99E-04	6.99E-04	6.99E-04	6.99E-04	6.99E-04
grey body irradiance [pW/mm^2]				2.61E-02	2.61E-02	2.61E-02	2.61E-02	2.61E-02
total flux at PACS detector [pW]				9.46E-05	9.46E-05	9.46E-05	9.46E-05	9.46E-05
% of standard telescope emission				2.29E-06	2.29E-06	2.29E-06	2.29E-06	2.29E-06
Emission from Cryocover Mirror Tube	1.117E-04	1	0.4329					
temperature T [K]				5	5	86	199	13
FBI integral for PACS 177 µm band				4.57E-04	4.57E-04	2.79E-02	3.08E-03	1.47E-01
grey body irradiance [pW/mm^2]				7.01E-03	7.01E-03	3.75E+04	1.19E+05	1.03E+02
total flux at SPIRE detector [pW]				7.83E-07	7.83E-07	4.18	13.24	0.01
% of standard telescope emission				1.90E-08	1.90E-08	0.10	0.32	0.0003
Gap between EB TUBE and IS TUBE	4.467E-04	1	0.4329					
temperature T [K]				40	38	38	75	80
FBI integral for PACS 177 µm band				1.37E-01	1.48E-01	1.48E-01	3.86E-02	3.32E-02
grey body irradiance [pW/mm^2]				8.61E+03	7.60E+03	7.60E+03	3.00E+04	3.34E+04
total flux at PACS detector [pW]				3.847	3.394	3.394	13.406	14.908
% of standard telescope emission				0.093	0.082	0.082	0.325	0.361

Table 5 (continued on next page)

LOU window emission through HiFi M3	2.892E-04	0.00046	0.9					
temperature T [K]				293	293	293	293	293
FBI integral for PACS 177 µm band				1.04E-03	1.04E-03	1.04E-03	1.04E-03	1.04E-03
grey body irradiance [pW/mm^2]				3.90E+05	3.90E+05	3.90E+05	3.90E+05	3.90E+05
total flux at PACS detector [pW]				0.0519	0.0519	0.0519	0.0519	0.0519
% of standard telescope emission				0.00126	0.00126	0.00126	0.00126	0.00126
LOU windows (all) through TS2/HIFI	5.82E-09	0.00451	0.9					
temperature T [K]				293	293	293	293	293
FBI integral for PACS 177 µm band				1.04E-03	1.04E-03	1.04E-03	1.04E-03	1.04E-03
grey body irradiance [pW/mm^2]				3.90E+05	3.90E+05	3.90E+05	3.90E+05	3.90E+05
total flux at PACS detector [pW]				0.00001	0.00001	0.00001	0.00001	0.00001
% of standard telescope emission				0.000000	0.000000	0.000000	0.000000	0.000000
Emission via gap below IS, holes in OB	3.626E-03	0.06285	0.9					
temperature T [K]				11	11	11	11	11
FBI integral for PACS 177 µm band				9.29E-02	9.29E-02	9.29E-02	9.29E-02	9.29E-02
grey body irradiance [pW/mm^2]				69.4	69.4	69.4	69.4	69.4
total flux at PACS detector [pW]				0.016	0.016	0.016	0.016	0.016
% of standard telescope emission				0.00038	0.00038	0.00038	0.00038	0.00038
Emission from LOU via gap below IS	3.626E-03	0.00451	0.9					
temperature T [K]				293	293	293	293	293
FBI integral for PACS 177 µm band				1.04E-03	1.04E-03	1.04E-03	1.04E-03	1.04E-03
grey body irradiance [pW/mm^2]				3.90E+05	3.90E+05	3.90E+05	3.90E+05	3.90E+05
total flux at PACS detector [pW]				6.384	6.384	6.384	6.384	6.384
% of standard telescope emission				0.155	0.155	0.155	0.155	0.155
LOU via gap between ENB and IS	4.467E-04	0.01766	0.9					
temperature T [K]				293	293	293	293	293
FBI integral for PACS 177 µm band				1.04E-03	1.04E-03	1.04E-03	1.04E-03	1.04E-03
grey body irradiance [pW/mm^2]				390123.4	390123.4	390123.4	390123.4	390123.4
total flux at PACS detector [pW]				3.077	3.077	3.077	3.077	3.077
% of standard telescope emission				0.074	0.074	0.074	0.074	0.074
TSE flux at PACS full field [pW]				**40.7**	**37.0**	**298.8**	**1542.4**	**126.9**
TSE in % of standard telescope				**0.99**	**0.90**	**7.23**	**37.34**	**3.07**
5% additional for diffraction				0.05	0.04	0.36	1.87	0.15
30% additional for misalignment				0.30	0.27	2.17	11.20	0.92
total TSE incl. diffr. + misalignm.				**1.33**	**1.21**	**9.77**	**50.41**	**4.15**

Table 5 continued: Thermal self emission contributors calculated for PACS 177 µm waveband.

case according to table 3 of RD4 : contributions to thermal self-emission	A eff [mm^2]	GCF	ε [0..1]	static 1 T [K]	static 2 T [K]	static 3 T [K]	static 4 T [K]	static 5 T [K]
Standard telescope	5.64	1	0.0150					
temperature T [K]				70	70	70	70	70
FBI integral for SPIRE 230 µm band				2.43E-02	2.43E-02	2.43E-02	2.43E-02	2.43E-02
grey body irradiance [pW/mm^2]				496.67	496.67	496.67	496.67	496.67
total flux at SPIRE detector [pW]				2802.71	2802.71	2802.71	2802.71	2802.71
% of standard telescope emission				100	100	100	100	100
Emission from CCM	2.87	1	ε [T]:	0.0010	0.0010	0.0013	0.0023	0.0010
temperature T [K]				11	5	86	199	13
FBI integral for SPIRE 230 µm band				1.78E-01	5.40E-03	1.45E-02	1.48E-03	2.21E-01
grey body irradiance [pW/mm^2]				0.15	0.00	59.28	301.10	0.36
total flux at SPIRE detector [pW]				0.42	0.00055	170.01	863.56	1.03
% of standard telescope emission				0.0151	0.000020	6.07	30.81	0.04
Emission from warm CVV	2.14E-03	1	0.04329					
temperature T [K]				293	293	293	293	293
FBI integral for SPIRE 230 µm band				4.89E-04	4.89E-04	4.89E-04	4.89E-04	4.89E-04
grey body irradiance [pW/mm^2]				8854.21	8854.21	8854.21	8854.21	8854.21
total flux at SPIRE detector [pW]				18.966	18.966	18.966	18.966	18.966
% of standard telescope emission				0.677	0.677	0.677	0.677	0.677
Gap CVV / TS2 baffle (crown)	1.42E-03	1	0.04329					
temperature T [K]				40	38	38	75	80
FBI integral for SPIRE 230 µm band				8.55E-02	9.45E-02	9.45E-02	2.05E-02	1.74E-02
grey body irradiance [pW/mm^2]				537.44	483.67	483.67	1591.59	1751.14
total flux at SPIRE detector [pW]				0.765	0.688	0.688	2.265	2.492
% of standard telescope emission				0.027	0.025	0.025	0.081	0.089
Emission from TS 2 Baffle tube	6.71E-03	1	0.4329					
temperature T [K]				40	38	38	75	80
FBI integral for SPIRE 230 µm band				8.55E-02	9.45E-02	9.45E-02	2.05E-02	1.74E-02
grey body irradiance [pW/mm^2]				5374.42	4836.68	4836.68	15915.93	17511.38
total flux at SPIRE detector [pW]				36.035	32.430	32.430	106.716	117.414
% of standard telescope emission				1.286	1.157	1.157	3.808	4.189
Emission from gap below IS	3.41E-03	1	0.9					
temperature T [K]				5.2	5.2	5.2	5.2	5.2
FBI integral for SPIRE 230 µm band				7.29E-03	7.29E-03	7.29E-03	7.29E-03	7.29E-03
grey body irradiance [pW/mm^2]				0.27	0.27	0.27	0.27	0.27
total flux at SPIRE detector [pW]				0.00093	0.00093	0.00093	0.00093	0.00093
% of standard telescope emission				0.000033	0.000033	0.000033	0.000033	0.000033
Emission from Cryocover Mirror Tube	3.66E-03	1	0.4329					
temperature T [K]				5	5	86	199	13
FBI integral for SPIRE 230 µm band				5.40E-03	5.40E-03	1.45E-02	1.48E-03	2.21E-01
grey body irradiance [pW/mm^2]				0.083	0.083	19440.51	56920.08	154.85
total flux at SPIRE detector [pW]				0.00030	0.00030	71.11	208.21	0.57
% of standard telescope emission				0.000011	0.000011	2.5	7.4	0.020
Gap between EB TUBE and IS TUBE	7.19E-04	1	0.4329					
temperature T [K]				40	38	38	75	80
FBI integral for SPIRE 230 µm band				8.55E-02	9.45E-02	9.45E-02	2.05E-02	1.74E-02
grey body irradiance [pW/mm^2]				5374.42	4836.68	4836.68	15915.93	17511.38
total flux at SPIRE detector [pW]				3.863	3.477	3.477	11.440	12.587
% of standard telescope emission				0.138	0.124	0.124	0.408	0.449

Table 6 (continued on next page)

LOU window emission through HiFi M3	3.47E-04	0.00046	0.9					
temperature T [K]				293	293	293	293	293
FBI integral for SPIRE 230 µm band				4.89E-04	4.89E-04	4.89E-04	4.89E-04	4.89E-04
grey body irradiance [pW/mm^2]				1.84E+05	1.84E+05	1.84E+05	1.84E+05	1.84E+05
total flux at SPIRE detector [pW]				0.0294	0.0294	0.0294	0.0294	0.0294
% of standard telescope emission				0.0010	0.0010	0.0010	0.0010	0.0010
LOU windows (all) through TS2/HIFI	3.94E-07	0.00451	0.9					
temperature T [K]				293	293	293	293	293
FBI integral for SPIRE 230 µm band				4.89E-04	4.89E-04	4.89E-04	4.89E-04	4.89E-04
grey body irradiance [pW/mm^2]				1.84E+05	1.84E+05	1.84E+05	1.84E+05	1.84E+05
total flux at SPIRE detector [pW]				0.00033	0.00033	0.00033	0.00033	0.00033
% of standard telescope emission				0.000012	0.000012	0.000012	0.000012	0.000012
Emission via gap below IS, holes in OB	3.41E-03	0.06285	0.9					
temperature T [K]				11	11	11	11	11
FBI integral for SPIRE 230 µm band				1.78E-01	1.78E-01	1.78E-01	1.78E-01	1.78E-01
grey body irradiance [pW/mm^2]				132.8	132.8	132.8	132.8	132.8
total flux at SPIRE detector [pW]				0.028	0.028	0.028	0.028	0.028
% of standard telescope emission				0.0010	0.0010	0.0010	0.0010	0.0010
Emission from LOU via gap below IS	3.41E-03	0.00451	0.9					
temperature T [K]				293	293	293	293	293
FBI integral for SPIRE 230 µm band				4.89E-04	4.89E-04	4.89E-04	4.89E-04	4.89E-04
grey body irradiance [pW/mm^2]				1.84E+05	1.84E+05	1.84E+05	1.84E+05	1.84E+05
total flux at SPIRE detector [pW]				2.834	2.834	2.834	2.834	2.834
% of standard telescope emission				0.101	0.101	0.101	0.101	0.101
LOU via gap between ENB and IS	7.19E-04	0.01766	0.9					
temperature T [K]				293	293	293	293	293
FBI integral for SPIRE 230 µm band				4.89E-04	4.89E-04	4.89E-04	4.89E-04	4.89E-04
grey body irradiance [pW/mm^2]				1.84E+05	1.84E+05	1.84E+05	1.84E+05	1.84E+05
total flux at SPIRE detector [pW]				2.336	2.336	2.336	2.336	2.336
% of standard telescope emission				0.083	0.083	0.083	0.083	0.083
TSE flux at SPIRE full field [pW]				**65.3**	**60.8**	**301.9**	**1216.4**	**158.3**
TSE in % of standard telescope				**2.33**	**2.17**	**10.77**	**43.40**	**5.65**
5% additional for diffraction				0.12	0.11	0.54	2.17	0.28
30% additional for misalignment				0.70	0.65	3.23	13.02	1.69
total TSE incl. diffr. + misalignm.				**3.14**	**2.93**	**14.54**	**58.59**	**7.62**

Table 6 continued: Thermal self emission contributors calculated for SPIRE 230 µm waveband.

case according to table 3 of RD4 : contributions to thermal self-emission	A eff [mm^2]	GCF	ε [0..1]	static 1 T [K]	static 2 T [K]	static 3 T [K]	static 4 T [K]	static 5 T [K]
Standard telescope	5.64	1	0.0150					
temperature T [K]				70	70	70	70	70
FBI integral for SPIRE 550 µm band				2.40E-03	2.40E-03	2.40E-03	2.40E-03	2.40E-03
grey body irradiance [pW/mm^2]				49.09	49.09	49.09	49.09	49.09
total flux at SPIRE detector [pW]				277.03	277.03	277.03	277.03	277.03
% of standard telescope emission				100	100	100	100	100
Emission from CCM	2.87	1	ε [T]:	0.0010	0.0010	0.0013	0.0023	0.0010
temperature T [K]				11	5	86	199	13
FBI integral for SPIRE 550 µm band				1.72E-01	2.02E-01	1.35E-03	1.19E-04	1.35E-01
grey body irradiance [pW/mm^2]				0.14	0.0071	5.52	24.28	0.22
total flux at SPIRE detector [pW]				0.41	0.020	15.82	69.65	0.63
% of standard telescope emission				0.148	0.0074	5.71	25.14	0.23
Emission from warm CVV	2.14E-03	1	0.04329					
temperature T [K]				293	293	293	293	293
FBI integral for SPIRE 550 µm band				3.80E-05	3.80E-05	3.80E-05	3.80E-05	3.80E-05
grey body irradiance [pW/mm^2]				687.55	687.55	687.55	687.55	687.55
total flux at SPIRE detector [pW]				1.47	1.47	1.47	1.47	1.47
% of standard telescope emission				0.53	0.53	0.53	0.53	0.53
Gap CVV / TS2 baffle (crown)	1.42E-03	1	0.04329					
temperature T [K]				40	38	38	75	80
FBI integral for SPIRE 550 µm band				1.10E-02	1.26E-02	1.26E-02	1.98E-03	1.65E-03
grey body irradiance [pW/mm^2]				69.02	64.27	64.27	153.92	166.17
total flux at SPIRE detector [pW]				0.098	0.091	0.091	0.219	0.236
% of standard telescope emission				0.035	0.033	0.033	0.079	0.085
Emission from TS 2 Baffle tube	6.71E-03	1	0.4329					
temperature T [K]				40	38	38	75	80
FBI integral for SPIRE 550 µm band				1.10E-02	1.26E-02	1.26E-02	1.98E-03	1.65E-03
grey body irradiance [pW/mm^2]				690.24	642.70	642.70	1539.17	1661.69
total flux at SPIRE detector [pW]				4.63	4.31	4.31	10.32	11.14
% of standard telescope emission				1.67	1.56	1.56	3.73	4.02
Emission from gap below IS	3.41E-03	1	0.9					
temperature T [K]				5.2	5.2	5.2	5.2	5.2
FBI integral for SPIRE 550 µm band				2.11E-01	2.11E-01	2.11E-01	2.11E-01	2.11E-01
grey body irradiance [pW/mm^2]				7.88	7.88	7.88	7.88	7.88
total flux at SPIRE detector [pW]				0.027	0.027	0.027	0.027	0.027
% of standard telescope emission				0.010	0.010	0.010	0.010	0.010
Emission from Cryocover Mirror Tube	3.66E-03	1	0.4329					
temperature T [K]				5	5	86	199	13
FBI integral for SPIRE 550 µm band				2.02E-01	2.02E-01	1.35E-03	1.19E-04	1.35E-01
grey body irradiance [pW/mm^2]				3.09	3.09	1809.00	4590.58	94.56
total flux at SPIRE detector [pW]				0.01	0.01	6.62	16.79	0.35
% of standard telescope emission				0.004	0.004	2.4	6.1	0.125
Gap between EB TUBE and IS TUBE	7.19E-04	1	0.4329					
temperature T [K]				40	38	38	75	80
FBI integral for SPIRE 550 µm band				1.10E-02	1.26E-02	1.26E-02	1.98E-03	1.65E-03
grey body irradiance [pW/mm^2]				690.24	642.70	642.70	1539.17	1661.69
total flux at SPIRE detector [pW]				0.50	0.46	0.46	1.11	1.19
% of standard telescope emission				0.18	0.17	0.17	0.40	0.43

Table 7 (continued on next page)

LOU window emission through HiFi M3	3.47E-04	0.00046	0.9					
temperature T [K]				293	293	293	293	293
FBI integral for SPIRE 550 µm band				3.80E-05	3.80E-05	3.80E-05	3.80E-05	3.80E-05
grey body irradiance [pW/mm^2]				1.43E+04	1.43E+04	1.43E+04	1.43E+04	1.43E+04
total flux at SPIRE detector [pW]				2.28E-03	2.28E-03	2.28E-03	2.28E-03	2.28E-03
% of standard telescope emission				8.24E-04	8.24E-04	8.24E-04	8.24E-04	8.24E-04
LOU windows (all) through TS2/HIFI	3.94E-07	0.00451	0.9					
temperature T [K]				293	293	293	293	293
FBI integral for SPIRE 550 µm band				3.80E-05	3.80E-05	3.80E-05	3.80E-05	3.80E-05
grey body irradiance [pW/mm^2]				1.43E+04	1.43E+04	1.43E+04	1.43E+04	1.43E+04
total flux at SPIRE detector [pW]				2.54E-05	2.54E-05	2.54E-05	2.54E-05	2.54E-05
% of standard telescope emission				9.17E-06	9.17E-06	9.17E-06	9.17E-06	9.17E-06
Emission via gap below IS, holes in OB	3.41E-03	0.06285	0.9					
temperature T [K]				11	11	11	11	11
FBI integral for SPIRE 550 µm band				1.72E-01	1.72E-01	1.72E-01	1.72E-01	1.72E-01
grey body irradiance [pW/mm^2]				128.9	128.9	128.9	128.9	128.9
total flux at SPIRE detector [pW]				0.028	0.028	0.028	0.028	0.028
% of standard telescope emission				0.010	0.010	0.010	0.010	0.010
Emission from LOU via gap below IS	3.41E-03	0.00451	0.9					
temperature T [K]				293	293	293	293	293
FBI integral for SPIRE 550 µm band				3.80E-05	3.80E-05	3.80E-05	3.80E-05	3.80E-05
grey body irradiance [pW/mm^2]				14294.3	14294.3	14294.3	14294.3	14294.3
total flux at SPIRE detector [pW]				0.22	0.22	0.22	0.22	0.22
% of standard telescope emission				0.079	0.079	0.079	0.079	0.079
LOU via gap between ENB and IS	7.19E-04	0.01766	0.9					
temperature T [K]				293	293	293	293	293
FBI integral for SPIRE 550 µm band				3.80E-05	3.80E-05	3.80E-05	3.80E-05	3.80E-05
grey body irradiance [pW/mm^2]				14294.3	14294.3	14294.3	14294.3	14294.3
total flux at SPIRE detector [pW]				0.181	0.181	0.181	0.181	0.181
% of standard telescope emission				0.065	0.065	0.065	0.065	0.065
TSE flux at SPIRE full field [pW]				**7.6**	**6.8**	**29.2**	**100.0**	**15.5**
TSE in % of standard telescope				**2.73**	**2.46**	**10.55**	**36.10**	**5.59**
5% additional for diffraction				0.14	0.12	0.53	1.81	0.28
30% additional for misalignment				0.82	0.74	3.17	10.83	1.68
total TSE incl. diffr. + misalignm.				**3.69**	**3.33**	**14.24**	**48.74**	**7.54**
measured value acc. to table 3 of RD5				$< 2 \cdot 10^{-14}$ W	$< 2 \cdot 10^{-14}$ W	3.5-5 %st	18-20 %st	6-8 % st
ratio of area field / area pixel:			57					
measuredTSE flux per pixel [pW]				**0.02**	**0.02**			
measured TSE flux at full field [pW]				1.14	1.14			
measured TSE in % stand. tel.				0.412	0.412	**4.25**	**19.0**	**7.0**
ratio measured / predicted				0.11	0.12	0.30	0.39	0.93

Table 7 continued: Thermal self emission contributors calculated for SPIRE 550 µm waveband.

case according to table 3 of RD4 :		static 1	static 2	static 3	static 4	static 5

contributions to thermal self-emission	A eff [mm^2]	GCF	ε [0..1]	T [K]	T [K]	T [K]	T [K]	T [K]
Standard telescope	5.64	1	0.0150					
temperature T [K]				70	70	70	70	70
FBI integral for PACS 88 µm band				1.38E-03	1.38E-03	1.38E-03	1.38E-03	1.38E-03
grey body irradiance [pW/mm^2]				28.18	28.18	28.18	28.18	28.18
total flux at SPIRE detector [pW]				159.03	159.03	159.03	159.03	159.03
% of standard telescope emission				100	100	100	100	100
Emission from CCM	2.87	1	ε [T]:	0.0010	0.0010	0.0013	0.0023	0.0010
temperature T [K]				11	5	86	199	13
FBI integral for SPIRE 670 µm band				1.28E-01	2.38E-01	7.68E-04	6.67E-05	9.51E-02
grey body irradiance [pW/mm^2]				0.11	0.01	3.14	13.59	0.15
total flux at SPIRE detector [pW]				0.31	0.02	9.02	38.96	0.44
% of standard telescope emission				0.19	0.02	5.67	24.50	0.28
Emission from warm CVV	2.14E-03	1	0.0433					
temperature T [K]				293	293	293	293	293
FBI integral for SPIRE 670 µm band				2.12E-05	2.12E-05	2.12E-05	2.12E-05	2.12E-05
grey body irradiance [pW/mm^2]				383.66	383.66	383.66	383.66	383.66
total flux at SPIRE detector [pW]				0.822	0.822	0.822	0.822	0.822
% of standard telescope emission				0.517	0.517	0.517	0.517	0.517
Gap CVV / TS2 baffle (crown)	1.42E-03	1	0.0433					
temperature T [K]				40	38	38	75	80
FBI integral for SPIRE 670 µm band				6.50E-03	7.46E-03	7.46E-03	1.13E-03	9.44E-04
grey body irradiance [pW/mm^2]				40.85	38.18	38.18	88.12	94.93
total flux at SPIRE detector [pW]				0.058	0.054	0.054	0.125	0.135
% of standard telescope emission				0.037	0.034	0.034	0.079	0.085
Emission from TS 2 Baffle tube	6.71E-03	1	0.4329					
temperature T [K]				40	38	38	75	80
FBI integral for SPIRE 670 µm band				6.50E-03	7.46E-03	7.46E-03	1.13E-03	9.44E-04
grey body irradiance [pW/mm^2]				408.49	381.84	381.84	881.24	949.29
total flux at SPIRE detector [pW]				2.739	2.560	2.560	5.909	6.365
% of standard telescope emission				1.722	1.610	1.610	3.716	4.002
Emission from gap below IS	3.41E-03	1	0.9					
temperature T [K]				5.2	5.2	5.2	5.2	5.2
FBI integral for SPIRE 670 µm band				2.41E-01	2.41E-01	2.41E-01	2.41E-01	2.41E-01
grey body irradiance [pW/mm^2]				9.00	9.00	9.00	9.00	9.00
total flux at SPIRE detector [pW]				0.031	0.031	0.031	0.031	0.031
% of standard telescope emission				0.019	0.019	0.019	0.019	0.019
Emission from Cryocover Mirror Tube	3.66E-03	1	0.4329					
temperature T [K]				5	5	86	199	13
FBI integral for SPIRE 670 µm band				2.38E-01	2.38E-01	7.68E-04	6.67E-05	9.51E-02
grey body irradiance [pW/mm^2]				3.65	3.65	1031.05	2568.20	66.69
total flux at SPIRE detector [pW]				0.01	0.01	3.77	9.39	0.24
% of standard telescope emission				0.008	0.008	2.4	5.9	0.153
Gap between EB TUBE and IS TUBE	7.19E-04	1	0.4329					
temperature T [K]				40	38	38	75	80
FBI integral for SPIRE 670 µm band				6.50E-03	7.46E-03	7.46E-03	1.13E-03	9.44E-04
grey body irradiance [pW/mm^2]				408.49	381.84	381.84	881.24	949.29
total flux at SPIRE detector [pW]				0.294	0.274	0.274	0.633	0.682
% of standard telescope emission				0.185	0.173	0.173	0.398	0.429

Table 8 (continued on next page)

LOU window emission through HiFi M3	3.47E-04	0.00046	0.9					
temperature T [K]				293	293	293	293	293
FBI integral for SPIRE 670 µm band				2.12E-05	2.12E-05	2.12E-05	2.12E-05	2.12E-05
grey body irradiance [pW/mm^2]				7.98E+03	7.98E+03	7.98E+03	7.98E+03	7.98E+03
total flux at SPIRE detector [pW]				1.27E-03	1.27E-03	1.27E-03	1.27E-03	1.27E-03
% of standard telescope emission				8.01E-04	8.01E-04	8.01E-04	8.01E-04	8.01E-04
LOU windows (all) through TS2/HIFI	3.94E-07	0.00451	0.9					
temperature T [K]				293	293	293	293	293
FBI integral for SPIRE 670 µm band				2.12E-05	2.12E-05	2.12E-05	2.12E-05	2.12E-05
grey body irradiance [pW/mm^2]				7.98E+03	7.98E+03	7.98E+03	7.98E+03	7.98E+03
total flux at SPIRE detector [pW]				1.42E-05	1.42E-05	1.42E-05	1.42E-05	1.42E-05
% of standard telescope emission				8.92E-06	8.92E-06	8.92E-06	8.92E-06	8.92E-06
Emission via gap below IS, holes in OB	3.41E-03	0.06285	0.9					
temperature T [K]				11	11	11	11	11
FBI integral for SPIRE 670 µm band				1.28E-01	1.28E-01	1.28E-01	1.28E-01	1.28E-01
grey body irradiance [pW/mm^2]				95.9	95.9	95.9	95.9	95.9
total flux at SPIRE detector [pW]				0.021	0.021	0.021	0.021	0.021
% of standard telescope emission				0.013	0.013	0.013	0.013	0.013
Emission from LOU via gap below IS	3.41E-03	0.00451	0.9					
temperature T [K]				293	293	293	293	293
FBI integral for SPIRE 670 µm band				2.12E-05	2.12E-05	2.12E-05	2.12E-05	2.12E-05
grey body irradiance [pW/mm^2]				7976.4	7976.4	7976.4	7976.4	7976.4
total flux at SPIRE detector [pW]				0.123	0.123	0.123	0.123	0.123
% of standard telescope emission				0.077	0.077	0.077	0.077	0.077
LOU via gap between ENB and IS	7.19E-04	0.01766	0.9					
temperature T [K]				293	293	293	293	293
FBI integral for SPIRE 670 µm band				2.12E-05	2.12E-05	2.12E-05	2.12E-05	2.12E-05
grey body irradiance [pW/mm^2]				7976.4	7976.4	7976.4	7976.4	7976.4
total flux at SPIRE detector [pW]				0.101	0.101	0.101	0.101	0.101
% of standard telescope emission				0.064	0.064	0.064	0.064	0.064
TSE flux at SPIRE full field [pW]				**4.5**	**4.0**	**16.8**	**56.1**	**9.0**
TSE in % of standard telescope				**2.83**	**2.53**	**10.55**	**35.29**	**5.64**
5% additional for diffraction				0.14	0.13	0.53	1.76	0.28
30% additional for misalignment				0.85	0.76	3.16	10.59	1.69
total TSE incl. diffr. + misalignm.				**3.83**	**3.42**	**14.24**	**47.64**	**7.61**

Table 8 continued: Thermal self emission contributors calculated for SPIRE 670 µm waveband.

5.2 Hot black body source illumination

The test conditions during STM2 test are described in RD3. Test results can be found in RD4.

The results for the external load cases (chopped hot black body source) as well as a comparison to the measured results are given in the following Table 9. Off-axis positions have not been simulated since the flux on SPIRE detector is already negligible for the centred position.

case according to table 3 of RD4			chopped 1	chopped 2	chopped 3	chopped 4	chopped 5	chopped 6
hot black body source position:			centred on LO band 3 window; distance 379 mm	15 mm (+Z) off-axis, distance 379 mm	30 mm (+Z) off-axis, distance 379 mm	LO band 3 taped	centred on left alignment window; distance 379 mm	centred on right alignment window; distance 379 mm
contributions to thermal self-emission	A eff [mm^2]	ε [0..1]	T [K]	T [K]	T [K]	T [K]	T [K]	T [K]
standard telescope	5.64	0.0150						
temperature T [K]			70	70	70	70	70	70
FBI integral for SPIRE band 550 µm			2.40E-03	2.40E-03	2.40E-03	2.40E-03	2.40E-03	2.40E-03
grey body irradiance [pW/mm^2]			49.09	49.09	49.09	49.09	49.09	49.09
total flux at SPIRE detector [pW]			277.03	277.03	277.03	277.03	277.03	277.03
% of standard telescope emission			100	100	100	100	100	100
HBB source through TS2 baffle and HIFI band 3	3.516E-09	1						
temperature T [K]			1473	1473	1473	1473	1473	1473
FBI integral for SPIRE band			2.00E-07	2.00E-07	2.00E-07	2.00E-07	2.00E-07	2.00E-07
grey body irradiance [pW/mm^2]			53347.9					
total flux at SPIRE detector [pW]			0.000188	no prediction	no prediction	no prediction	no prediction	no prediction
% of standard telescope emission			0.000068					
predicted total TSE flux at SPIRE full field [pW]			**1.9E-04**					
predicted total TSE in % of standard telescope			**0.0000677**					
ratio of area full field/area pixel:		57						
measured value TSE flux at SPIRE per pixel [pW]					**0.0005**	**0.0005**	**0.0005**	**0.0005**
measured TSE flux at SPIRE full field [pW]					0.03	0.03	0.03	0.03
measured TSE in % of standard telescope			**0.0009**	**0.0006**	0.01	0.01	0.01	0.01
ratio measured / predicted			13.3					

Table 9 Dynamic (chopped) cases: emission from external hot black body source

5.3 Summary of predicted results

For the static load cases the prediction is in reasonably good agreement with the measurements. Table 7 contains a comparison of predictions for the static load cases to measured values as obtained during STM2 stray light test, see row “ratio measured/predicted”.

For the external illumination (chopped) cases a slightly larger deviation of predicted from measured stray light levels was found for the chopped case 1 with a hot blackbody source located 379 mm in front of the LO window of HIFI channel 3 (the other cases have not been simulated). Results are given in Table 9 of section 5.2.

The attenuation within the HIFI FPU is shown in the following table. It is roughly estimated as the ratio of effective source areas traced from the LO windows and from the HIFI M3 mirror to the SPIRE detector.

Ray trace from LO windows to SPIRE detector	3.94E-07	mm^2
Ray trace from HIFI M3 to SPIRE detector	3.47E-04	mm^2
attenuation within HIFI from ray tracing	1.14E-03	

Table 10 Attenuation within HIFI

Note: The attenuation which was finally taken for the in-orbit prediction was 0.01 (see RD6, page 57).

E N D O F D O C U M E N T

	Name	Dep./Comp.		Name	Dep./Comp.
	Alberti von Mathias Dr.	ASG22		Steininger Eric	AED32
	Barlage Bernhard	AED13	x	Stritter Rene	AED11
	Bayer Thomas	ASA42		Suess Rudi	OTN/ASA44
	Brune Holger	ASA45		Thörmer Klaus-Horst Dr.	OTN/AED65
	Edelhoff Dirk	AED2		Wagner Klaus	ASG22
	Fehringer Alexander	ASG13	x	Wietbrock Walter	AET12
x	Fricke Wolfgang Dr.	AED 65		Wöhler Hans	ASG22
	Geiger Hermann	ASA42		Wössner Ulrich	ASE252
	Grasl Andreas	OTN/ASA44			
	Grasshoff Brigitte	AET12			
			x	Alcatel Alenia Space Cannes	ASP
	Hauser Armin	ASG22	x	ESA/ESTEC	ESA
	Hendry David	Terma			
	Hengstler Reinhold	ASA42		**Instruments:**	
	Hinger Jürgen	ASG22	x	MPE (PACS)	MPE
x	Hohn Rüdiger	AED65	x	RAL (SPIRE)	RAL
x	Hölzle Edgar Dr.	AED32	x	SRON (HIFI)	SRON
	Huber Johann	ASA42		**Subcontractors:**	
	Hund Walter	ASE252		Air Liquide, Space Department	AIR
x	Idler Siegmund	AED312		Air Liquide, Space Department	AIRS
	Ivády von András	FAE12		Air Liquide, Orbital System	AIRT
	Jahn Gerd Dr.	ASG22		Alcatel Alenia Space Antwerp	ABSP
	Kalde Clemens	ASM2		Austrian Aerospace	AAE
	Kameter Rudolf	OTN/ASA42		Austrian Aerospace	AAEM
	Kettner Bernhard	AET42		APCO Technologies S. A.	APCO
	Knoblauch August	AET32		Bieri Engineering B. V.	BIER
	Koelle Markus	ASA43		BOC Edwards	BOCE
	Koppe Axel	AED312		Dutch Space Solar Arrays	DSSA
x	Kroeker Jürgen	AED65		EADS Astrium Sub-Subsyst. & Equipment	ASSE
	La Gioia Valentina	Terma		EADS CASA Espacio	CASA
	Lamprecht Ernst	OTN/ASQ22		EADS CASA Espacio	ECAS
	Lang Jürgen	ASE252		EADS Space Transportation	ASIP
	Langenstein Rolf	AED15		Eurocopter	ECD
	Langfermann Michael	ASA41		European Test Services	ETS
	Mattia Stefano	Terma		HTS AG Zürich	HTSZ
	Much Christoph	ASA43		Linde	LIND
	Müller Jörg	ASA42		Patria New Technologies Oy	PANT
	Müller Martin	ASA43		Phoenix, Volkmarsen	PHOE
	Peltz Heinz-Willi	ASG13		Prototech AS	PROT
	Pietroboni Karin	AED65		QMC Instruments Ltd.	QMC
	Platzer Wilhelm	AED2		Rembe, Brilon	REMB
	Reichle Konrad	ASA42		Rosemount Aerospace GmbH	ROSE
	Runge Axel	OTN/ASA44		RYMSA, Radiación y Microondas S.A.	RYM
x	Schink Dietmar	AED32		SENER Ingenieria SA	SEN
	Schlosser Christian	OTN/ASA44		Stöhr, Königsbrunn	STOE
	Schmidt Rudolf	FAE12		Terma A/S, Herlev	TER
	Schweickert Gunn	ASG22		Terma A/S, Herlev	TERM